Available online at www.sciencedirect.com

ScienceDirect

Procedia Structural Integrity 26 (2020) 3–10

Structural Integrity Procedia

www.elsevier.com/locate/procedia

The 1st Mediterranean Conference on Fracture and Structural Integrity, MedFract1

Luminescence efficiency of CaF_2:Eu single crystals: Temperature dependence

George Saatsakis[a], Konstantinos Ninos[b], Ioannis Valais[c], Niki Martini[c], Nektarios Kalyvas[c], Charilaos Kantsos[b], Athanasios Bakas[b], Ioannis Kandarakis[c], George Panayiotakis[a], Christos Michail[c,*]

[a]*University of Patras, School of Medicine, Department of Medical Physics, GR-15310, Rion, Greece*
[b]*University of West Attica, Department of Biomedical Sciences, Athens 12210, Greece*
[c]*University of West Attica, Radiation Physics, Department of Biomedical Engineering, Materials Technology and Biomedical Imaging Laboratory, Athens 12210, Greece*

Abstract

During the last decades, there is increasing interest in applications of scintillators at harsh environments (i.e., high temperatures or radiation fluxes), such as in geophysical detectors for deep geology boreholes, non-destructive testing (NDT) of pipelines in oil and gas industry, space and marine exploration, nuclear reactor monitoring, radiation chemistry, etc. To this aim, the current study is the first step towards the investigation of the luminescence efficiency dependence of single-crystal scintillators over wide temperature ranges. Calcium fluoride doped with europium (CaF_2:Eu) was selected due to the fact that it has a high melting point at 1418°C and is also robust to mechanical and thermal shocks. The dimensions of the single-crystal sample were 10x10x10 mm^3 , and it was irradiated using typical X-ray radiographic exposures (90 kVp, 63mAs) in order to measure the light photon intensity dependence with temperature (22 to 128 °C). The luminescence efficiency was found maximum at the lowest examined temperature (22.01 efficiency units-E.U. at 22 °C-environmental). With increasing temperature, the luminescence efficiency decreased almost exponentially due to thermal quenching (4.43 efficiency units-E.U. at 128 °C).

Keywords: Inorganic Scintillators; Single Crystals; Radiation detectors; CaF_2:Eu, Temperature dependence

* Corresponding author. Tel.: +0030-210-5385387
E-mail address: cmichail@upatras.gr

10.1016/j.prostr.2020.06.002

1. Introduction

Scintillators, coupled with optical sensors, are used in various applications in order to convert radiation to light (Salomoni et al. 2018, Maddalena et al. 2019). Frequently used crystals are sodium iodide activated with thallium-NaI:Tl, Bismuth Germinate Oxide-BGO, Yttrium Orthoaluminate Perovskite-YAP, Lutetium Oxyorthosilicate-LSO, Gadolinium Oxyorthosilicate-GSO among others (Melcher et al. 1991, Van Eijk 2002, Michail et al. 2016b, Karpetas et al. 2017, Kilian et al. 2018). Traditionally, they are used in applications, such as high energy physics, homeland security and in medical imaging (i.e., X-ray computed tomography-CT, positron emission tomography-PET, positron emission mammography-PEM, radiotherapy, radiography, mammography, etc.) (Valentine et al. 1993, Nikl et al. 2006, Ogino et al. 2006, Mares et al. 2007, Kamada et al. 2008, Kytyr et al. 2010, Mikhailik and Kraus 2010a, Yanagida et al. 2010, Alenkov et al. 2011, Blahuta et al. 2011, Yoshikawa et al. 2011, Drozdowski et al. 2012, Mares et al. 2012, Michail et al. 2016a, Michail et al. 2018a, Hu et al. 2019, Martini et al. 2019, Mykhaylyk et al. 2019).

Besides these applications, scintillators are used for non-destructive testing (NDT) of welds on pipelines and pressure vessels in the oil and gas industry. In such applications as well as, in deep geology boreholes, marine research, nuclear plants, space exploration, the measurement of the ionizing radiation is subject to extreme conditions (pressure, temperature, etc.) (Melcher et al. 1991, Zee et al. 2001, Aksnes 2009, Legrand 2012, Bulatovic et al. 2013, Marek et al. 2013, Rothkirch et al. 2013, de Faoite et al. 2015, Bisong et al. 2019, Lebedev et al. 2019, Patri et al. 2019, Saxena et al. 2019). Due to these limitations, the detectors that will be used should have properties like adequate light output under elevated temperature, chemical stability, mechanical properties, and energy resolution for such conditions (Yang et al. 2014).

An alternative scintillator is europium-activated calcium fluoride (CaF_2:Eu), that has been used, in single crystal and nanocrystal forms, for medical physics and spectroscopy applications, charged particle detection, in the search for dark matter, in low-energy radiation detectors, solar cell application, homeland security, etc. (Holl et al. 1988, Bernabei et al. 1997, Knoll 2000, Ely et al. 2005, Wang et al. 2005, Bensalaha et al. 2006, Hong et al. 2007, Chen 2008, Shimizu et al. 2008, Wang et al. 2009, Mikhailik and Kraus 2010b, Song et al. 2010, Cappella et al. 2013, Plettner et al. 2013, Lina et al. 2015, Salah et al. 2015, Lecoq et al. 2017, Cortelletti et al. 2018, Dujardin et al. 2018, Fan et al. 2018, Yanagida 2018). CaF_2:Eu can be easily found in nature and can be manufactured in large quantities at a low cost. Europium-activated calcium fluoride is easily machined, offers excellent operational characteristics, such as non-hygroscopicity, inertness, insolubility, and thus can be placed in direct contact with solvent systems (solubility 0.0017g/100g H_2O) or aqueous solutions (Table 1).

Table 1. CaF_2:Eu single-crystal intrinsic and mechanical properties (data obtained from Advatech website).

Properties Scintillator/Optical	Units	Value	Properties Mechanical	Units	Value
Wavelength (Max. Emission)	Nm	435	Density	g/cm³	3.18
Wavelength Range	Nm	395 – 525	Atomic Number (Effective)		16.5
Decay Time	Ns	950	Melting Point	ºK	1360
Light Yield	photons/keV	30	Linear Expansion Coefficient	C^{-1}	19.5×10^{-6}
Photoelectron Yield	% of NaI(Tl)	50	Thermal Conductivity	$Wm^{-1}K^{-1}$	9.7
Radiation Length	Cm	3.05	Crystal Structure		Cubical
Optical Transmission	μm	0.13 -10μm	Hardness	Mho	4
Transmittance	%	TBA	Hygroscopic		No
Refractive Index		1.47 (@ 435nm)	Solubility	g/100gH_2 0	0.0017
Reflection Loss/Surface	%	5.4			

When used in particle or low energy radiation detectors, it exhibits good mechanical properties; in combination with its very low vapour pressure, it is well suited for use within vacuums. Its robustness to thermal and mechanical shock, with a high melting point (1418°C), is an essential fact for extreme environmental applications. The low inherent background radiation of CaF_2:Eu is also another important characteristic. The energy resolution is 5.7-6.07 % at 662 keV for a scintillator with such a low-Z. The energy resolution of CaF_2:Eu does not degrade noticeably with temperature. Thus, investigation of this crystals for harsh environmental applications could be of interest (Heath et al. 1979, Holl et al. 1988, Belli et al. 1999, Knoll 2000, Maushake 2008, Shimizu et al. 2008, Plettner et al. 2013, Sasidharan et al. 2013, Nakamura et al. 2017, Wang et al. 2018).

The purpose of the present study was to investigate the temperature dependence of a CaF_2:Eu single crystal, under X-ray excitation, for applications of detectors in harsh environments (temperature or radiation flux) (Rutherford et al. 2016). To this aim, experimental measurements of the absolute luminescence efficiency (AE-light energy flux over exposure rate) were performed under typical X-ray excitation in X-ray radiographic exposures (Koukou et al. 2015) in order to measure the light photon intensity dependence with temperature.

2. Materials and methods

The CaF_2:Eu single crystal sample was purchased from Advatech UK Limited with dimensions 10x10x10mm (Advatech 2020). All crystal sample surfaces were polished. The crystal was exposed to X-rays on a BMI General Medical Merate tube with rotating Tungsten anode and inherent filtration equivalent to 2 mm Al, at typical radiographic energy (90 kVp, 63mAs) in order to measure the light photon intensity dependence with temperature (22 to 128 °C). An additional 20 mm filtration was introduced in the beam to simulate beam quality alternation by the human body (Michail et al. 2018b). The crystal sample was heated using a Perel 3700-9 2000W heating gun up to 128°. The temperature on the crystal surface was monitored using an Extech RH101 infrared digital thermometer (0.1% accuracy).

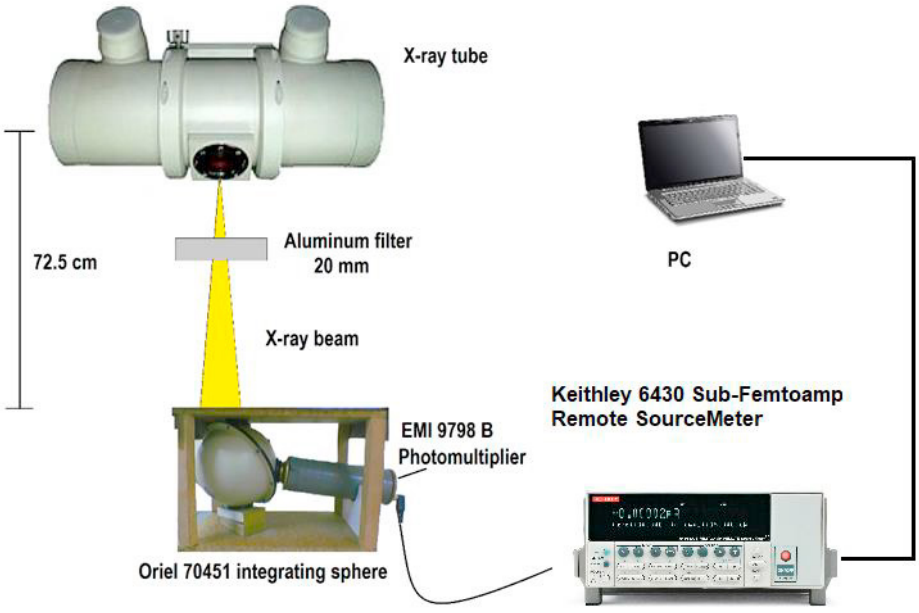

Fig. 1. Experimental setup for the X-ray irradiation of the heated CaF_2:Eu single crystal.

2.1. Absolute Luminescence Efficiency

The light emission efficiency of a phosphor may be experimentally estimated under X-ray imaging conditions, by determining the absolute luminescence efficiency (AE) defined by (2.1) (Michail et al. 2019):

$$\eta_{\mathrm{A}} = \dot{\Psi}_{\lambda} / \dot{X} \tag{1}$$

where $\dot{\Psi}_{\lambda}$ is the emitted light energy flux (energy of light per unit of area and time), $\dot{X}$ is the incident exposure rate that excites the phosphor to luminescence. AE is traditionally expressed in units of $\mu W \times m^{-2} /(mR \times s^{-1})$ thereafter referred to as efficiency units (E.U.). The S.I. equivalent of this unit is given in $\mu W \times m^{-2} /(mGy \times s^{-1})$, where mGy stands for the corresponding air Kerma. The light flux measurements were performed using an experimental set up comprising a light integration sphere (Oriel 70451) coupled to a photomultiplier (PMT) (EMI 9798B), which was connected to a Cary 401 vibrating reed electrometer. The photomultiplier was coupled to the output port of the integrating sphere in order to reduce experimental errors due to illumination non-uniformities. The crystal was positioned at the input port of the integrating sphere, whereas the photomultiplier was adapted at the output port (Fig. 1) (Michail et al. 2010). The photocathode of the photomultiplier (extended S-20) was directly connected to a Keithley Model 6430 Sub-Femtoamp Remote SourceMeter (Keithley Instruments Inc., Cleveland, OH, USA) electric current meter (Saatsakis et al. 2019).

The light flux of the screens was finally determined after corrections on the experimental data according to the following formula:

$$\dot{\Psi}_{\Lambda} = \frac{I_{elec}}{\tau_0 (s_{PC} a_s)} \cdot \frac{1}{A_{sc}} \tag{2}$$

I_{elec} is the current at the output of the electrometer (in pA), s_{PC} is the peak photosensitivity of the photocathode (in pA/W), which was used as a factor converting the output photocathode current into light energy flux. a_s is the spectral matching factor of the screen's emission spectrum to the spectral sensitivity of the photocathode (extended S-20) used to correct for the spectral mismatches between the emitted light and the spectral sensitivity of the photocathode (extended S-20) of the photomultiplier. A_{sc} is the irradiated area of the screen. τ_0 denotes the throughput of the integrating sphere, which is expressed by the ratio:

$$\tau_0 = \frac{\Psi_e}{\Psi_i} = \frac{\rho_o A_e / A_{sc}}{(1 - \rho_o (1 - A_p / A_{sc}))} \tag{3}$$

Ψe is the total light flux at the exit (output) port of the integrating sphere, Ψi is the total flux at the input port, A_e is the area of the exit port, A_p is the sum of all port areas, and ρ_0 denotes the reflectance of the internal sphere wall. Using the setup of Fig. 1 and prototype light-emitting diodes (LED, Kingbright Company), the total throughput of the apparatus was calculated by also taking into account specific data on A_e, A_{sc}, A_p,ρ_0) given by the manufacturer's datasheet. The estimated throughput value was then τ_0=15.6.

3. Results and discussion

Table 2 shows quality control results on the X-ray unit that was used for the experimental procedure. For all measurements 1 second of irradiation at 63 mAs was maintained. Tube voltage was varied from 50 to 130 kVp, and an external aluminum filtration of 20 mm was used. As can be depicted from Table 2, the kVp accuracy of the radiographic X-ray tube is below 3.5% well within the suggested limits (European Union 2012, AAPM 2015).

Figure 2 shows absolute luminescence efficiency results for the examined crystal sample at various temperatures (22 to 128 °C). This temperature range is indicative since, for example, crystals in logging detectors are subjected to temperatures from below 0 °C to above 200 °C Melcher et al. (1991). Exposure of the scintillator to excessive heating or X-ray flux can result in crystal cracking (Pokluda et al. 2015, Kastengren 2019).

As can be depicted from Figure 2, the luminescence efficiency is temperature dependent (Kastengren 2019). The luminescence efficiency decreases with increasing temperature since light output is also affected by radiation-less transitions whose probability increase with temperature (Melcher et al. 1991). Furthermore, possible impurities and lattice defects, reduce the scintillation signal.

Table 2. X-ray Tube output measurements with the Piranha (RTI) dosimeter.

kVp nominal	kVp measured	msec	mGy	mGy/sec	HVL	Total filtration (mm)
50	49.59	999.2	0.03586	0.03583	4.41	23
60	60.59	999.2	0.1146	0.1144	5.58	22
70	69.92	999.2	0.2481	0.2478	6.65	24
80	80.68	999.2	0.4522	0.4514	7.53	22
90	91.68	999.7	0.7323	0.7314	8.36	22
100	101.64	999.2	1.086	1.083	9.05	23
110	111.9	999.2	1.512	1.507	9.68	23
120	122.98	999.2	2.016	2.011	10.3	24
130	126.02	999.7	2.275	2.269	10.4	24

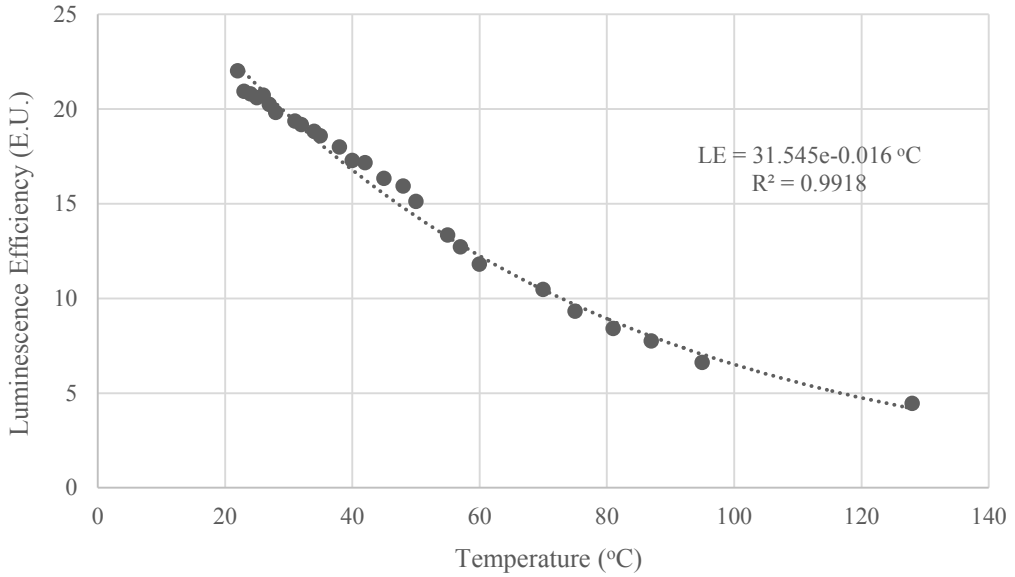

Fig. 2. Absolute luminescence efficiency of the heated CaF_2:Eu single crystal (90 kVp).

This is important, especially in applications requiring crystals of large dimensions. The luminescence efficiency was found maximum at the lowest examined temperature (22.01 efficiency units-E.U. at 22 °C-environmental). With increasing temperature, the luminescence efficiency decreased almost exponentially due to thermal quenching (4.43 efficiency units-E.U. at 128 °C). These results are indicative of the performance of the crystals in applications in harsh environments, such as in space exploration. For example, spacecraft which approach the Sun should be extremely resource limited in both mass and power since they will face harsh environments (radiation levels and increased temperature) regarding the onboard instrumentation. In this case, detectors that need little or no cooling, lasting on high radiation fluxes, will be able to succeed in the mission goals.

4. Conclusion

In this research, an initial investigation of the effect of temperature on the luminescence efficiency properties of Calcium Fluoride (Eu) single crystal scintillators, for applications in harsh environments, was performed. From the measured luminescence efficiency values, a decrease of the order of almost 80% was observed when the crystal surface was heated to the maximum temperature value of this experiment. Thus, it is crucial to use crystals showing

resistance to high temperatures for various applications. Further experimentation of such scintillating materials to temperatures above and way below the temperatures incorporated in this initial research, need to be carried out in order to establish their effectiveness in applications under harsh temperature conditions.

References

AAPM Report No 151: Ongoing Quality Control in Digital Radiography, The Report of AAPM Imaging Physics Committee, Task Group 151, February 2015.

Advatech UK. CaF_2(Eu) - Calcium Fluoride (Eu). Available online: https://www.advatech-uk.co.uk/caf2_eu.html (accessed on 25-01-2020).

Aksnes, A., 2009. Photonic Sensors for Health and Environmental Monitoring, in *"*Proceedings of the NATO Advanced Study Institute Sensors for Environment, Health and Security Advanced Materials and Technologies*"*. In: Baraton, M. (Ed.). Springer, The Netherlands, pp. 191.

Alenkov, V., Buzanov, O. Khanbekov, N., Kim, S., Kim, H., Kornoukhov, V., Kraus, H., Mikhailik, V., 2011. Growth and characterization of isotopically enriched $^{40}Ca_{100}MoO_4$ single crystals for rare event search experiments. Crystal and Research Technology 46(12) 1223-1228.

Belli, P., Bernabei, R., Dai, C., Grianti, F., He, H., Incicchitti, A., Kuang, H., Ma, J., Montecchia, F., Ignesti, G., Ponkratenko, O., Prosperi, D., Tretyak, V., Zdesenko. Y., 1999. New limits on spin-dependent coupled WIMPs and on 2β processes in ^{40}Ca and ^{46}Ca by using low radioactive CaF_2(Eu) crystal scintillators. Nuclear Physics B 563, 97-106.

Bensalaha, A., Mortiera, M., Patriarcheb, G., Gredinc, P., Viviena, D., 2006. Synthesis and optical characterizations of undoped and rare-earth-doped CaF_2 nanoparticles. Journal of Solid State Chemistry 179, 2636-2644.

Bernabei, R., Belli, P., Montecchia, F., Incicchitti, A., Nicolantonio, W., Prosperi, D., Bacci, C., Dai, C., Ding, L., Kuang, H.,Ma, J., Yao, Z., 1997. Improved limits on WIMP-^{19}F elastic scattering and first limit on the 2EC2v ^{40}Ca decay by using a low radioactive CaF_2(Eu) scintillator. Astroparticle Physics 7, 73-76.

Bisong, M., Mikhailov, V., Lepov, V., Makharova, S., 2019. Microstructure influence on crack resistance of steels welded structures operated in an extremely cold environment. Procedia Structural Integrity 20, 37-41.

Blahuta, S., Bessière, A., Viana, B., Ouspenski, V., Mattmann, E., Lejay, J., Gourier, D., 2011. Defects Identification and Effects of Annealing on $Lu_{2(1-x)}Y_2xSiO_5$ (LYSO) Single Crystals for Scintillation Application. Materials 4, 1224-1237.

Bulatovic, S., Aleksic, V. and Milovic, L., 2013. Failure of steam line causes determined by NDT testing in power and heating plants. Frattura ed Integrità Strutturale, 7(26), 41-48.

Cappella, F., Bernabei, R., Belli, P., Caracciolo, V., Cerulli, R., Danevich, F., d'Angelo, A., Di Marco, A., Incicchitti, A., Poda, D., Tretyak, V., 2013. On the potentiality of the $ZnWO_4$ anisotropic detectors to measure the directionality of Dark Matter. The European Physical Journal C 73, 2276.

Chen, M., 2008. Double beta decay: Scintillators. Journal of Physics: Conference Series 136, 022035.

Cortelletti, P., Pedroni, M., Boschi, F., Pin, S., Ghigna, P., Canton, P., Vetrone, F., Speghini, A., 2018. Luminescence of Eu^{3+} Activated CaF_2 and SrF_2 Nanoparticles: Effect of the Particle Size and Codoping with Alkaline Ions. Crystal Growth & Design 18, 686-694.

de Faoite, D., Hanlon, L., Roberts, O., Ulyanov, A., McBreen, S., Tobin, I., Stanton, K., 2015. Development of glass-ceramic scintillators for gamma-ray astronomy. Journal of Physics: Conference Series 620, 012002.

Drozdowski, W., Brylew, K., Chruścińska, A., Kamada, K., Yanagida, T., Yoshikawa, A., 2012. Scintillation yield enhancement in LuAG:Pr crystals following thermal annealing. Optical Materials 34(12), 1975-1978.

Dujardin, C., Auffray, E., Bourret-Courchesne, E., Dorenbos, P., Lecoq, P., Nikl, M., Vasil'ev, A., Yoshikawa, A., Zh, R., 2018. Needs, Trends, and Advances in Inorganic Scintillators. IEEE Transactions on Nuclear Science 65, 1977-1997.

Ely, J., Aalseth, C., McIntyre, J., 2005. Novel beta-gamma coincidence measurements using phoswich detectors. Journal of Radioanalytical and Nuclear Chemistry 263, 245-250.

European Commission, Radiation protection N° 162: Criteria for Acceptability of Medical Radiological Equipment used in Diagnostic Radiology, Nuclear Medicine and Radiotherapy, Directorate-General for Energy Directorate D - Nuclear Safety & Fuel Cycle Unit D4 - Radiation Protection, 2012 Luxembourg: Publications Office of the European Union, 2012.

Fan, T., Lü, J., Huang, Y., Li, G., 2018. Monodispersing Eu^{3+} and Li+ codoped CaF_2 nanoparticles for efficient luminescence. Micro Nano Letters 13, 393-396.

Heath, R., Hofstadter, R., Hughes, E., 1979. Inorganic scintillators: A review of techniques and applications. Nuclear Instruments and Methods 162, 431-476.

Holl, I., Lorenz, E., Mageras, G, 1988. A Measurement of the Light Yield of Common Inorganic Scintillators. IEEE Transactions on Nuclear Science 35(1), 105-109.

Hong, B., Kawano, K., 2007. Syntheses of Eu-Activated Alkaline Earth Fluoride MF_2 (M=Ca, Sr) Nanoparticles. Japanese Journal of Applied Physics 46(9B), 6319-6323.

Hu, Z., Chen, X., Chen, H., Shi, Y., Liu, X., Xie, T., Kou, H., Pan, Y., Mihokova, E., Nikl, M., Li, J., 2019. Suppression of the slow scintillation component of $Pr:Lu_3Al_50_{12}$ transparent ceramics by increasing Pr concentration. Journal of Luminescence 210, 14-20.

Kamada, K., Tsutsumi, K., Usuki, Y., Ogino, H., Yanagida, T., Yoshikawa, A., 2008. Crystal Growth and Scintillation Properties of 2-Inch-Diameter $Pr:Lu_3Al_5O_{12}$ (Pr:LuAG) Single Crystal. IEEE Transactions on Nuclear Science 55(3), 1488-1491.

Karpetas, G., Michail, C., Fountos, G., Kalyvas, N., Valais, I., Kandarakis, I., Panayiotakis, G., 2017. Detective Quantum Efficiency (DQE) in PET Scanners: A Simulation Study. Applied Radiations and Isotopes 125, 154-162.

Kastengren, A., 2019. Thermal behavior of single-crystal scintillators for high-speed X-ray imaging. Journal of Synchrotron Radiation 26, 205-214.

Kilian, A., Bilski, P., Gorbenko, V., Zorenko, T., Witkiewicz, S., Paprocki, K., Zorenko, Y., 2018. Thermoluminescent Properties of Cerium-Doped Lu_2SO_5 and Y_2SiO_5 Single Crystalline Films Scintillators Grown from $PbO-B_2O_3$ and Bi_2O_3 Fluxes. Crystals, 8, 120.

Knoll, G., 2000. Radiation Detection and Measurement. John Wiley and Sons.

Koukou, V., Martini, N., Michail, C., Sotiropoulou, P., Fountzoula, C., Kalyvas, N., Kandarakis, I., Nikiforidis, G., and Fountos, G., 2015. Dual energy method for breast imaging: A simulation study. Computational and Mathematical Methods in Medicine, 2015, 574238.

Kytyr, D., Doktor, T., Jirousek, O., Zlamal, P. and Pokorny, D., 2010. Experimental and numerical study of cemented bone-implant interface behavior. Frattura ed Integrità Strutturale 5(15), 5-13.

Lebedev, M., Startsev, O., Kychkin, A., 2019. Development of climatic tests of polymer materials for extreme operating conditions. Procedia Structural Integrity, 20, 81-86.

Lecoq, P., Gektin, A., Korzhik, M., 2017. Inorganic Scintillators for Detector Systems, Physical Principles and Crystal Engineering, Second Edition, Springer: Switcherland.

Legrand, V., 2012. Crystallography Under Extreme Conditions: State of the Art and Perspectives, Recent Advances in Crystallography, IntechOpen, 39-66. http://dx.doi.org/10.5772/48608.

Lina, L., Leitnera, D., Benattia, C., Perdikakis, G., Krausea, S., Rencsoka, R., Nasha, S., Wittmer, W., 2015. Investigation of ion induced damage in KBr, YAG:Ce, CaF_2:Eu and CsI:Tl irradiated by various-energy protons. Journal of Instrumentation 10, P03024.

Maddalena, F., Tjahjana, L., Xie, A., Arramel, A., Zeng, S., Wang, H., Coquet, P., Drozdowski, W., Dujardin, C., Dang, C., Birowosuto, M., 2019. Inorganic, Organic, and Perovskite Halides with Nanotechnology for High-Light Yield X- and γ-ray Scintillators. Crystals 9(2), 88.

Marek, T., Kubát, J., Malý, P., Nikl, M., 2013. Complex oxide scintillators for extreme conditions, IEEE, 3rd International Conference on Advancements in Nuclear Instrumentation, Measurement Methods and their Applications, pp. 1-4. doi: 10.1109/ANIMMA.2013.6727946

Mares, J., Beitlerova, A., Nikl, M., Vedda, A., D'Ambrosio, C., Blazek, K., Nejezchleb, K., 2007, Time development of scintillating response in Ce□ or Pr□ doped crystalsPhysica Status Solidi C 4(3), 996-999.

Mares, J., Nikl, M., Beitlerova, A., Horodysky, P., Blazek, K., Bartos, K., D'Ambrosio, C., 2012. Scintillation Properties of Ce^{3+}-and Pr^{3+}-Doped LuAG, YAG and Mixed Lu_xY_{1-x}AG Garnet Crystals. IEEE Transactions on Nuclear Science 59(5), 2120-2125.

Martini, N., Koukou, V., Fountos, G., Valais, I., Bakas, A., Ninos, K., Kandarakis, I., Panayiotakis, G., Michail, C., 2018. Towards the enhancement of medical imaging with non-destructive testing (NDT) CMOS sensors. Evaluation following IEC 62220-1-1:2015 international standard. Procedia Structural Integrity 10, 326-332.

Martini, N., Koukou, V., Fountos, G., Valais, I., Kandarakis, I., Michail, C., Bakas, A., Lavdas, E., Ninos, K., Oikonomou, G., Gogou, L. and Panayiotakis, G., 2019. Imaging performance of a $CaWO_4$/CMOS sensor. Frattura ed Integrità Strutturale 13(50) pp. 471-480.

Maushake, P., 2008. Calcium Fluoride Crystals. Optik & Photonik 2, 46-47.

Melcher, C., Schweitzer, J., Manente, R., Peterson, C., 1991. Applications of single crystals in oil well logging. Journal of Crystal Growth 109, 37-42.

Menefee, J., Sweinehart, C., O'Dell, E.,1966. Calcium fluoride as an x-ray and charged particle detector. IEEE Transactions on Nuclear Science N5-13(1), 720-724.

Mikhailik, V., Kraus, H., 2010. Performance of scintillation materials at cryogenic temperatures. Physics Status Solidi B 247(7), 1583-1599.

Mikhailik, V., Kraus, H., 2010. Scintillators for Cryogenic Applications: State-of-Art. Journal of Physical Studies 14 (4).

Michail, C., Fountos, G., Liaparinos, P., Kalyvas, N., Valais, I., Kandarakis, I., Panayiotakis, G., 2010. Light emission efficiency and imaging performance of Gd_2O_2S:Eu powder scintillator under X-ray Radiography conditions. Medical Physics, 37(7), 3694-3703.

Michail, C., Karpetas, G., Fountos, G., Kalyvas, N., Valais, I., Fountzoula, C., Zanglis, A., Kandarakis, I., Panayiotakis, G., 2016. A novel method for the Optimization of Positron Emission Tomography Scanners Imaging Performance. Hellenic Journal of Nuclear Medicine 19(3), 231-240.

Michail, C., Valais, I., Martini, N., Koukou, V., Kalyvas, N., Bakas, A., Kandarakis, I., Fountos, G., 2016. Determination of the Detective Quantum Efficiency (DQE) of CMOS/CsI Imaging Detectors following the novel IEC 62220-1-1:2015 International Standard. Radiation Measurements 94, 8-17.

Michail, C., Karpetas, G., Kalyvas, N., Valais, I., Kandarakis, I., Agavanakis, K., Panayiotakis, G., Fountos, G., 2018. Information Capacity of Positron Emission Tomography Scanners Crystals 8(12), 459.

Michail, C., Valais, I., Fountos, G., Bakas, A., Fountzoula, C., Kalyvas, N., Karabotsos, A., Sianoudis, I., Kandarakis, I., 2018. Luminescence Efficiency of Calcium Tungstate ($CaWO_4$) under X-ray radiation: Comparison with Gd_2O_2S:Tb. Measurement 120, 213-220.

Michail, C., Kalyvas, N., Bakas, A., Ninos, K., Sianoudis, I., Fountos, G., Kandarakis, I., Panayiotakis, G., Valais, I., 2019. Absolute Luminescence Efficiency of Europium-Doped Calcium Fluoride (CaF_2:Eu) Single Crystals under X-ray Excitation. Crystals 9(5), 234.

Mykhaylyk, V., Kraus, H., Salib, M., 2019. Bright and fast scintillation of organolead perovskite $MAPbBr_3$ at low temperatures. Materials Horizons, 6, 1740-1747.

Nakamura, F., Kato, T., Okada, G., Kawaguchi, N., Fukuda, K., Yanagida, T., 2017. Scintillation and dosimeter properties of CaF_2 translucent ceramic produced by SPS. Journal of the European Ceramic Society 37, 1707-1711.

Nikl, M., Pejchal, J., Mihokova, E., Mares, J., Ogino, H., Yoshikawa, A., Fukuda, T., Vedda, A., D'Ambrosio, C., 2006. Antisite defect-free $Lu_3(Ga_xAl_{1-x})_5O_{12}$:$PrLu_3(Ga_xAl_{1-x})_5O_{12}$:Pr scintillator. Applied Physics Letters 88, 141916.

Ogino, H., Yoshikawa, A., Nikl, M., Krasnikov, A., Kamada, K., Fukuda, T., 2006. Growth and scintillation properties of Pr-doped Lu. Journal of Crystal Growth 287, 335-338.

Patri, S. Kumar, H., Prasad, K., Meikandamurthy, C., Sreedhar, B., Vijayashree, R., Prakash, V., Selvaraj, P., 2019. Failure analysis of structural screw joint in a start-up neutron detector handling mechanism. Procedia Structural Integrity 14, 688-695.

Plettner, C., Pausch, G., Scherwinski, F., Herbach, C., Lentering, R., Kong, Y., Römer, K., Grodzicka, M., Szcześniak, T., Iwanowska, J., Moszyński, M., 2013. CaF_2(Eu): an "old" scintillator revisited. Journal of Instrumentation 8, P06010

Pokluda, J., Vojtek, T., Hohenwarter, A., Pippan, R., 2015. Effects of microstructure and crystallography on crack path and intrinsic resistance to shear-mode fatigue crack growth. Frattura ed Integrità Strutturale 34, 142-149.

Rothkirch, A., Diego Gatta, G., Meyer, M., Merkel, S., Merlini, M., Liermann, H., 2013. Single-crystal diffraction at the Extreme Conditions beamline P02.2: procedure for collecting and analyzing high-pressure single-crystal data. Journal of Synchrotron Radiation. 20, 711-720.

Rutherford, M., Chapman, D., White, T., Drakopoulos, M., Rack, A., Eakins, D., 2016. Evaluating scintillator performance in time-resolved hard X-ray studies at synchrotron light sources. Journal of Synchrotron Radiation 23, 685-693.

Saatsakis, G., Kalyvas, N., Michail, C., Ninos, K., Bakas, A., Fountzoula, C., Sianoudis, I., Karpetas, G., Fountos, G., Kandarakis, I., Valais, I., Panayiotakis, G., 2019. Optical Characteristics of ZnCuInS/ZnS (Core/Shell) Nanocrystal Flexible Films Under X-Ray Excitation. Crystals 9, 343.

Salah, N., Alharbi, N., Habib, S., Lochab, S., 2015. Luminescence Properties of CaF_2 Nanostructure Activated by Different Elements. Journal of Nanomaterials 2015, 136402.

Salomoni, M., Pots, R., Auffray, E., Lecoq, P., 2018. Enhancing Light Extraction of Inorganic Scintillators Using Photonic Crystals. Crystals 8(2), 78.

Sasidharan, S., Jayasree, A., Fazal, S., Koyakutty, M., Nair, S., Menon, D., 2013. Ambient temperature synthesis of citrate stabilized and biofunctionalized, fluorescent calcium fluoride nanocrystals for targeted labeling of cancer cells. Biomaterials Science 1, 294-305.

Saxena, A., 2019. Challenges in predicting crack growth in structures operating in extreme environments. Procedia Structural Integrity14, 774-781.

Shimizu, Y., Minowa, M., Suganuma, W., Inoue, Y., 2006. Dark matter search experiment with CaF_2(Eu) scintillator at Kamioka Observatory. Physics Letters B 633, 195-200.

Song, L., Gao, J., Song. R., 2010. Synthesis and luminescent properties of oleic acid (OA)-modified CaF_2:Eu nanocrystals. Journal of Luminescence 130, 1179-1182.

Valentine, J., Moses, W., Derenzo, S., Wehe, D., Knoll, G., 1993. Temperature dependence of CsI(Tl) gamma-ray excited scintillation characteristics. Nuclear Instruments and Methods in Physics Research Section A: Accelerators, Spectrometers, Detectors and Associated Equipment 325(1-2), 147-157.

Van Eijk, C., 2002. Inorganic scintillators in medical imaging. Physics in Medicine and Biology 47, R85-R106.

Wang, F., Fan, X., Pi, D., Wang, M., 2005. Synthesis and luminescence behavior of Eu^{3+}-doped CaF_2 nanoparticles. Solid State Communications 133, 775-779.

Wang, J., Miao, W., Li, Y., Yao, H., Li, Z., 2009. Water-soluble Ln^{3+}-doped calcium fluoride nanocrystals: Controlled synthesis and luminescence properties. Materials Letters 63, 1794-1796.

Wang, J., Yang, J., Hu, T., Chen, X., Lang, J., Wu, X., Zhang, J., Zhao, H., Yang, J., Cui, Q., 2018. Structural Phase Transition and Compressibility of CaF_2 Nanocrystals under High Pressure. Crystals 8(5), 199.

Yanagida, T., Yoshikawa, A., Yokota, Y., Kamada, K., Usuki, Y., Yamamoto, S., Miyake, M., Baba, M., Kumagai, K., Sasaki, K., Ito, M., Abe, N., Fujimoto, Y., Maeo, S., Furuya, Y., Tanaka, H., Fukabori, A., Rodrigues dos Santos, T., Takeda, M., Ohuchi, N., 2010. Development of Pr:LuAG Scintillator Array and Assembly for Positron Emission Mammography. IEEE Transactions on Nuclear Science 57(3), 1492-1495.

Yanagida, T., 2018. Inorganic scintillating materials and scintillation detectors. Proceedings of the Japan Academy, Ser. B 94, 75-97.

Yang, H., Peng, F., Zhang, Q., Guo, C., Shi, C., Liu, W., Sun, G., Zhao, Y., Zhang, D., Sun, D., Yin, S., Gu, M., Mao, R., 2014. A promising high-density scintillator of $GdTaO_4$ single crystal. CrystEngComm 16, 2480-2485.

Yoshikawa, A., Yanagida, T., Kamada, K., Yokota, Y., Pejchal, J., Usuki, Y., Yamamoto, S., Miyake, M., Kumagai, K., Yamaji, A., Sasaki, K., dos Santos, T., Baba, M., Ito, M., Takeda, M., Ohuchi, N., Nikl, M., 2010. Positron emission mammography using Pr:LuAG scintillator - Fusion of optical material study and systems engineering. Optical Materials 32,1294-1297.

Zee, R., Xiao, Z., Chin, B., Liu, J., 2001. Processing of single crystals for high temperature applications. Journal of Materials Processing Technology, 113(1-3), 75-80.